

Including atomic vibrations in XANES calculations: polarization-dependent damping of the fine structure at the Cu K edge of $(\text{creat})_2\text{CuCl}_4$

O. Šipr,^{1,*} J. Vackář,¹ and A. Kuzmin²

¹*Institute of Physics of the ASCR v. v. i., Cukrovarnická 10, CZ-162 53 Prague, Czech Republic*

²*Institute of Solid State Physics, University of Latvia, Kengaraga street 8, LV-1063 Riga, Latvia*

(Dated: September 24, 2018)

Atomic vibrations are usually not taken into account when analyzing x-ray absorption near edge structure (XANES) spectra. One of the reasons is that including the vibrations in a formally exact way is quite complicated while the effect of vibrations is supposed to be small in the XANES region. By analyzing polarized Cu K edge x-ray absorption spectra of creatinium tetrachlorocuprate $[(\text{creat})_2\text{CuCl}_4]$, we demonstrate that a technically simple method, consisting in calculating the XANES via the same formula as for static systems but with a modified free-electron propagator which accounts for fluctuations of interatomic distances, may substantially help in understanding XANES of some layered systems. In particular we show that the difference in the damping of the x-ray absorption fine structure oscillations for different polarisations of the incoming x-rays cannot be reproduced by calculations which rely on a static lattice but it can be described if atomic vibrations are accounted for in such a way that individual creatinium and CuCl_4 molecular blocks are treated as semi-rigid entities while the mutual positions of these blocks are subject to large mean relative displacements.

PACS numbers: 78.70.Dm

Keywords: XANES, vibrations, multiple-scattering formalism

I. INTRODUCTION

The importance of atomic vibrations for a proper description of x-ray absorption spectra (XAS) in the extended x-ray absorption fine structure (EXAFS) region has been recognised since the early years of this technique.^{1,2} The vibrations have to be accounted for to obtain a proper damping of x-ray absorption fine structure (XAFS) oscillations at high energies. Including the vibrations in XAS calculations is in general a difficult task because in principle one has to evaluate the spectrum for all possible geometric configurations (distributions of instantaneous positions of atoms) and to average the signals with proper weights. Doing this explicitly might be computationally very demanding so usually some further simplifications are invoked, such as assumption of a Gaussian or nearly-Gaussian distribution regarding the atomic positions and of validity of single-scattering and plane-wave approximations regarding the effect of vibrations on the photoelectron state.^{1,3} Sometimes, an explicit averaging of the XAFS signal has been employed as well — both when treating a thermal disorder^{4–7} and when treating a static disorder.^{4,7–9}

So far the attention has been focused mostly either on the pre-edge region or on the EXAFS region. The interest in the pre-edge region is driven mainly by the effort to explain the emergence of some pre-peaks as a consequence of a vibrational local symmetry breaking which allows some otherwise forbidden dipole transitions.^{10–12} The interest in the EXAFS region stems from the fact that accounting for vibrations is obligatory for an accurate fitting of EXAFS signal to extract reliable values of coordination numbers, bond lengths and mean-square relative displacements (MSRD's).^{2,7} The x-ray near-edge

structure (XANES) region covering photoelectron energies up to about 50 eV and the intermediate energy region (photoelectron energies 50–100 eV) have not attracted much attention in this respect. One of the reasons is that one expects the effect of vibrations to be small at low k -values close to the absorption edge, as it is reflected by the Debye-Waller factor $\exp(-2\sigma^2 k^2)$ which occurs in the conventional EXAFS formula.³ Besides, the use of the Fourier filtering procedure affects the quality of the EXAFS signal at low k -values, so that this part is usually excluded from the structural analysis.

However, there might be effects in the XANES or intermediate energy regions for which the vibrations could be important, and it would be useful to check it. Analysis of specific examples would certainly be quite instructive in this respect. An appealing option is to focus on polarised spectra of layered systems, because (i) polarised XANES contains significantly more information than orientationally-averaged spectra, meaning also that polarised XANES presents a much more stringent test to the theory^{13–15} and (ii) for layered systems is it more likely that the vibrations will damp different scattering signals in a different way, giving thus rise to features in the spectra which might not be possible to explain unless these vibrations are taken into account.

Including Gaussian or harmonic vibrations into EXAFS calculations is a relatively straightforward procedure, as long as we deal with energy region where single-scattering and plane-wave approximation can be used. Here, the main challenge is to find the vibrational modes of the system and to use them for obtaining the appropriate parameters *ab initio*.^{16–19}

Including vibrations into XANES calculations, where multiple-scattering effects have to be considered, is more

difficult because, among others, in this case one should deal with displacements of more than just two atoms at a time. One possible direction is to employ Taylor expansion around equilibrium positions to obtain usable formula for the statistical average of the signals for different geometric configurations. This approach was pursued by Benfatto *et al.*⁴ who started with analytic formula describing signals of order n and applied the expansion regarding both the free-electron propagator and the scattering phase shifts. A similar route was taken by Fujikawa *et al.*²⁰ who also applied Taylor expansion but this time regarding only the propagator.

Another possible approach is to rely on scattering path expansion to employ Debye-Waller damping factors specific for each scattering path.¹⁷ Similarly to the scheme of Benfatto *et al.*,⁴ this scheme is more suitable to the EXAFS than to the XANES because it can be used only if the scattering path expansion converges.²¹

Recently, the problem of calculating electronic structure for a system of vibrating atoms was formulated in the framework of alloy theory, by identifying each instantaneous atomic position with a new atomic type and treating the problem within the coherent potential approximation (CPA).²² Due to its general nature, this scheme could be applied to XAS. The CPA framework is quite powerful as it implicitly includes the effect of vibrations both on the propagator and on the phase shifts. On the other hand, because all atomic displacements are treated independently, this scheme cannot describe a situation where some atoms vibrate only a little relatively to each other but at the same time vibrate quite a lot relatively to other atoms, i.e., when both strongly correlated and uncorrelated atomic vibrations are present at the same time.

All these procedures have various degree of accuracy and sophistication and proved to be useful in various circumstances.^{22–26} At the same time, their implementation is not simple. It is noteworthy in this respect that even though methodological works undoubtedly present a significant progress,^{4,16–20} practical applications of these approaches to XANES calculations remain to be quite rare. A broader use of these techniques could be helped by demonstrating that useful results can be obtained even by simple implementations of the procedures mentioned above. If these techniques are to be used in the XANES region, one has to opt for a formulation which treats the multiple scattering exactly. On top of that, it would be convenient if correlations between movements of various atoms was taken into account to some extent. In this work we focus on testing a simplified version of the method of Fujikawa *et al.*,²⁰ which consists in calculating XANES by using essentially the same formula as for static systems, just with a modified free-electron propagator to account for pair-wise fluctuations of interatomic distances. Effectively this means that the multiple scattering is treated exactly while the effect of vibrations is treated within the plane wave approximation. Respective formulas were already incorporated earlier, e.g., in

the FEFF9 code.^{27,28} However, to the best of our knowledge they have not really been used for solving practical problems of XANES analysis so far.

We suggest that by means of the procedure outlined in Sec. II A one can describe experimentally observable trends that could not be described within the static lattice model. We demonstrate this on the case of Cu K edge spectra of (creat)₂CuCl₄. Copper K edge XAS of Cu-containing complexes was subject to intensive research in the past. There has been a still unsettled debate about the “local and many-body” or “delocalised and one-electron” interpretation of x-ray near-edge structure (XANES) at the Cu K edge in systems containing CuCl_{*n*} or CuO_{*n*} blocks.^{13–15,29–37} An important place in these discussion was given to the angular or polarisation dependence of the spectra close to the edge. However, not much attention has been paid to the polarisation dependence of XAFS further above the edge, for photoelectron energies 30–100 eV. A striking feature in this energy region is a big difference in how the XAFS oscillations are damped with the increasing energy for different polarisations of the incoming x-rays. We demonstrate in this work that these differences cannot be explained by calculations which rely on a static lattice. By including the vibrations in XANES calculations we show that the observed anisotropy of XAFS damping can be reproduced if the mean square relative displacements are chosen so that individual molecular blocks in the (creat)₂CuCl₄ crystal are treated as semi-rigid entities while the mutual positions of these blocks are subject to large disorder. Application of the procedure thus offers a view on the nature of vibrations in the material in question. It is especially suited for analysing XAFS of layered systems.

II. METHODS

A. Treatment of vibrations

We start by discussing an approach to account for atomic vibrations within the real space multiple-scattering formalism. Let us recall that for a static system, the XANES transition rate can be evaluated as^{21,38,39}

$$\mu(\hbar\omega) = -\frac{2\pi^2 m^2}{\hbar^5 k^2} \Im \sum_{LL'} M_L^* \tau_{LL'}^{00} M_{L'} \quad , \quad (1)$$

where $k = \sqrt{2m(\hbar\omega - E_0)/\hbar^2}$ is the photoelectron wave vector, M_L is the atomic-like transition matrix element and $\tau_{LL'}^{00}$ is the scattering-path operator comprising all the scattering events,

$$\tau_{LL'}^{00} = t_L^0 \delta_{LL'} + \sum_p \sum_{L''} t_L^0 G_{LL''}^{0p} \tau_{L''L'}^{p0} \quad . \quad (2)$$

The definitions of the single-site scattering matrix t_L^p and of the free-electron propagator $G_{LL''}^{pq}$ can be found in the

above mentioned reviews.^{21,38,39} The angular-momentum subscript L is an abbreviation for the pair (ℓ, m) and the sum \sum_p runs over all atoms in the cluster, with 0 denoting the photoabsorbing site.

The method we use for accounting for the vibrations is essentially the same as what was introduced by Fujikawa *et al.*²⁰ as “renormalisation of the scattering series by a plane wave thermal factor”. As mentioned in Sec. I, the formula was included also in the FEFF9 code^{27,28} but no discussion of it was given. The procedure consists in calculating the XANES using same formula as for static systems but replacing the free-electron propagator $G_{LL''}^{pq}$ in Eq. (2) according to

$$G_{LL''}^{pq} \rightarrow G_{LL''}^{pq} e^{-k^2 \sigma_{pq}^2}, \quad (3)$$

where σ_{pq}^2 is the MSRD characterising the fluctuations of the distance between the atoms p and q .

Fujikawa *et al.*²⁰ derived their formula by expanding the free-electron propagator — Eq. (3) above is equivalent to Eq. (3.18) in Ref. 20. (Note, however, that these authors used a more accurate and at the same time more complicated expression in their own application of this technique.)^{24,25} It is worthy to note that the *ansatz* Eq. (3) can be obtained also by another way, by means of exploiting the analogy with EXAFS formula. To show this, we start with the expression for EXAFS oscillations for static systems:³

$$\begin{aligned} \chi &\equiv \frac{\mu - \mu_0}{\mu_0} \\ &= \sum_p \frac{3(\hat{\boldsymbol{\varepsilon}} \cdot \hat{\mathbf{R}}_p)^2}{kR_p^2} \Im \left[f_p(k) e^{2ikR_p + 2i\delta_{\ell=1}^0} \right]. \end{aligned} \quad (4)$$

Here $\boldsymbol{\varepsilon}$ is the polarisation vector, R_p is the distance between the photoabsorbing atom and the atom p , $f_p(k)$ is the backward scattering amplitude, and $\delta_{\ell=1}^0$ is the scattering phase shift of the central atom ($\ell = 1$ in case of the K edge). For a vibrating system one can extend Eq. (4) to the well-known formula^{1,3}

$$\chi = \sum_p \frac{3(\hat{\boldsymbol{\varepsilon}} \cdot \hat{\mathbf{R}}_p)^2}{kR_p^2} \Im \left[f_p(k) e^{2ikR_p^0 + 2i\delta_{\ell=1}^0} e^{-2k^2 \sigma_p^2} \right]. \quad (5)$$

In deriving Eq. (5) from Eq. (4), one has to neglect the influence of vibrations on the electronic structure represented by $f_p(k)$ and $\delta_{\ell=1}^0$ and assume that the vibrations are harmonic. There is, however, yet another way to arrive at Eq. (5). Namely, one can start with the basic expression (1), perform the substitution (3) and only afterwards apply all the approximations which transform Eq. (1) into Eq. (4), namely, restrict the multiple scattering just to single scattering and apply the plane wave approximation to the free electron propagator.

Having this in mind, we can see that if one calculates XANES spectrum along the same procedures as in the static case with only performing the substitution (3), one gets XANES spectrum for a vibrating system, with the

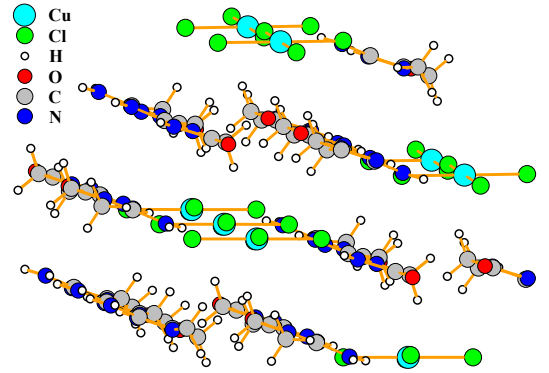


FIG. 1. Structural diagram of $(\text{creat})_2\text{CuCl}_4$. The z axis is perpendicular to the CuCl_4 blocks.

scattering events treated exactly and with the effects of vibrations treated approximatively. In particular, (i) the effect of vibrations is restricted to changes in the geometry, i.e., the scattering phase shifts are the same as for a static system, (ii) the effect of vibrations is restricted to varying the bond lengths for each pair independently, neglecting thus, among others, bond angles variations and (iii) the effect of vibrations is treated within the plane wave approximation (while the electron scattering itself and hence the bulk of the spectral shape are calculated exactly, i.e., with curved waves). It should be mentioned that correlations between movements of different atomic pairs can be included only partially, by a suitable choice of the MSRD for each pair, as it is done in Sec. III below.

We will show in the following that despite all the approximations the *ansatz* Eq. (3) can describe the effect of vibrations so that features seen in the experiment can be interpreted as arising from vibrations.

B. Technical details of XANES calculations

We apply the method outlined above to the Cu K edge XANES of $(\text{creat})_2\text{CuCl}_4$. The crystal structure of $(\text{creat})_2\text{CuCl}_4$ is monoclinic (crystal group 14). Lattice vectors lengths we use are $a=8.106$ Å, $b=7.835$ Å, $c=13.685$ Å, angles between the lattice vectors are $\alpha=90^\circ$, $\beta=114^\circ$, $\gamma=90^\circ$. A structural diagram is shown in Fig. 1. Most of the calculations presented here were performed within the real space multiple-scattering formalism,³⁹ using the RSMS code.^{40,41} We used a non-self-consistent muffin-tin potential constructed according to the Mattheiss prescription (superposition of potentials and charge densities of isolated atoms). To alleviate the deficiencies of the muffin-tin approximation, some calculations were done also while inserting additional “empty spheres” into the interstitial region. The positions and radii of these empty spheres were obtained via the XBAND code,⁴² relying on procedures commonly used in the linear muffin-tin orbital (LMTO) method

calculations.⁴³ The core hole left by the excited photoelectron was treated within the final state approximation (“relaxed and screened model”).^{14,38,39} The exchange and correlation effects were accounted for via an energy-independent $X\alpha$ potential with the Kohn-Sham value of $\alpha=0.67$. We do not employ energy-dependent exchange-correlation potential because there is no universal recipe which one to choose for a particular case.^{44–46} Our focus will be on the anisotropy of XAFS damping and selecting a different exchange-correlation potential would just shift the positions of all the peaks no matter to which polarization they belong, hence this is not really important for our study.

The XANES spectra presented in this work were obtained for clusters of radii of 7.8 Å (185 atoms including H atoms, 103 atoms disregarding H atoms). Fairly well size-converged spectra were obtained already for clusters of radii of 4.5 Å (33 atoms including H atoms, 19 atoms disregarding H atoms). Constructing the muffin-tin potential for hydrogen atoms has been problematic sometimes.⁴⁷ However, in our case this is not an issue because we checked that the spectra calculated with H atoms included and with H atoms ignored are practically identical.

Raw spectra were broadened by an energy-dependent Lorentzian to simulate the combined effect of the experimental resolution, of the decay of the core hole and of the decay of the excited photoelectron. The constant part of the broadening was set to 1.50 eV, the energy-dependent part of the broadening was set to $0.08E$, where E is the photoelectron energy. Such a choice leads to reasonable spectra. The agreement between theory and experiment could further be improved by optimizing the broadening function.^{48,49} While such a procedure is useful when structural optimization is sought, in our case it would have no influence on the conclusions because we focus on the *differences* in XAFS damping for different polarizations while the Lorentzian broadening is isotropic.

C. Plane-waves calculations

Band-structure calculations relying on plane waves basis set and pseudopotentials were performed using the ABINIT code.⁵⁰ First, self-consistent calculation was done using 16 \mathbf{k} -points in the irreducible Brillouin zone. Afterwards, angular-momentum-projected density of states (DOS) within a sphere around the Cu atom with radius of 1.24 Å was calculated using 38 \mathbf{k} -points. The cut-off energy for the plane waves was set to 40 H. All these parameters were checked for convergence. The core hole was ignored. The results presented here were obtained using a Hartwigsen-Goedecker-Hutter type pseudopotentials available at the ABINIT web-site.⁵¹ We verified that very similar results are obtained also for pseudopotentials of the Troullier-Martins type.^{52,53}

Because of the use of pseudopotentials, we did not have access to the core wave functions and, consequently, we

were not able to calculate XANES spectra directly. However, if the core hole is neglected and dipole selection rule is invoked, polarised XANES spectra can be taken as proportional to the appropriate angular-momentum component of the projected DOS multiplied by a smooth function which corresponds to the square of the atomic transition matrix element M_L . The proportionality between XAS and DOS is, strictly speaking, true only under specific symmetry requirements which guarantee that the scattering path operator τ_{LL}^{00} , entering Eq. (1) is diagonal. However, in most cases this is fulfilled with sufficient accuracy. We checked explicitly using the RSMS code that XAS and DOS are indeed proportional in our case. Having all this in mind, we obtained XANES spectra via ABINIT simply by taking the projected DOS and multiplying it by a smooth sinusoidal-like function which increases monotonously from 1.0 at the absorption edge to 1.6 at the end of the energy region we cover. We chose this particular form of the DOS-to-XAS proportionality function just for convenience, our conclusions are not dependent on it. Polarisation-sensitivity of the spectra was achieved by taking the ($\ell=1, m=0$) DOS component to get the XANES with the $\varepsilon\parallel z$ polarisation and the ($\ell=1, m=\pm 1$) DOS component to get the XANES with the $\varepsilon\perp z$ polarisation. The same convolution of the raw results by an energy-dependent Lorentzian curve was applied as in case of real-space multiple-scattering calculations.

III. APPLICATION TO THE CU K EDGE XAS OF $(\text{CREAT})_2\text{CuCl}_4$

In the following we will demonstrate the potential of the procedure outlined in Sec. II A by analysing the Cu K edge XAS of $(\text{creat})_2\text{CuCl}_4$. The experimental spectrum taken from the work of Kosugi *et al.*³⁰ is shown in the second from the bottom panel of Fig. 2. The polarisation vector of the incoming x-rays either lies in the plane defined by the photoabsorbing Cu atom and its four nearest Cl neighbours ($\varepsilon\perp z$) or is perpendicular to this plane ($\varepsilon\parallel z$, cf. Fig. 1). Unlike most of previous works on the Cu K edge XAS of $(\text{creat})_2\text{CuCl}_4$, our focus is not on the first 10 eV above the edge but on the higher energy region, in particular on the strong suppression of the fine structure for the $\varepsilon\parallel z$ spectrum for energies 20 eV and more above the edge.

A. Calculations relying on a static lattice

First we find out whether the anisotropic damping of XAFS oscillations can be reproduced by calculations done for a static crystal. Theoretical spectra obtained using the RSMS code are shown above the experimental spectrum in Fig. 2, spectrum obtained using the ABINIT code is shown below the experimental spectrum. Spectra labelled $\varepsilon\parallel z$ were calculated for linearly polarised x-rays,

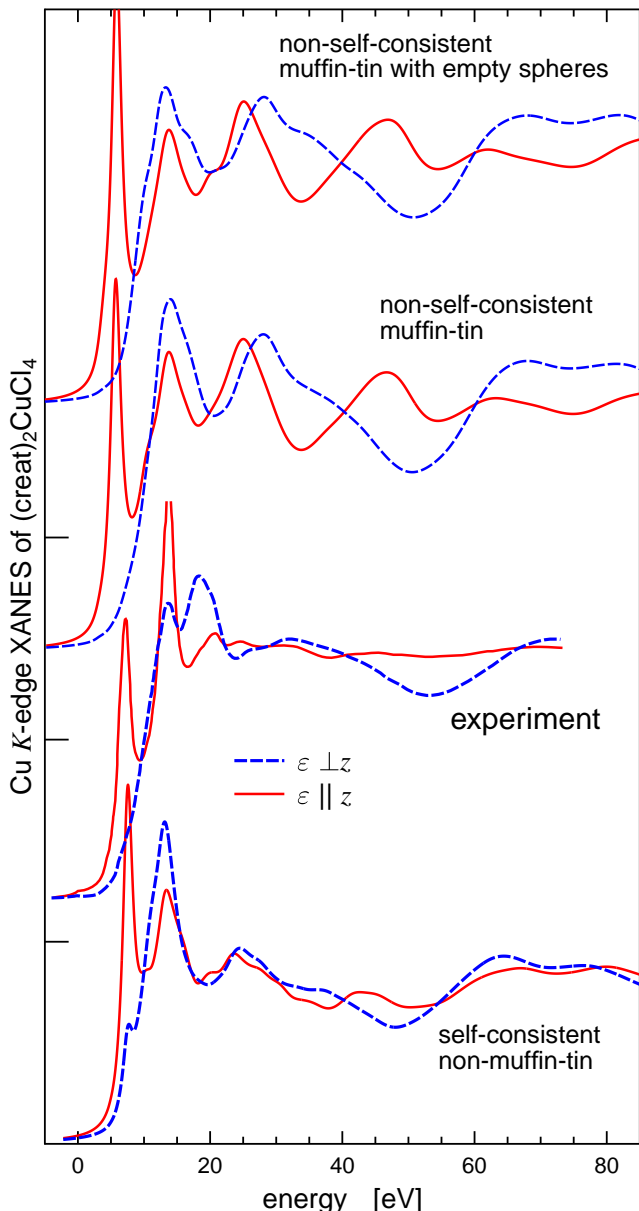


FIG. 2. Experimental polarised Cu K edge XANES of $(\text{creat})_2\text{CuCl}_4$ (Ref. 30) compared to spectra calculated for a static crystal. The two uppermost panels display spectra obtained via the RSMS code, the lowermost panel displays spectra obtained via the ABINIT code. The origin of the energy scale is arbitrary.

spectra labelled $\varepsilon \perp z$ were calculated for circularly polarised x-rays. The horizontal alignment of the spectra was done by hand so that the position of the peak around 12 eV for $\varepsilon \parallel z$ matches the experiment.

It is evident that none of the calculations describes the suppression of the fine structure for $\varepsilon \parallel z$. In particular, this is true for calculations which use a non-self-consistent potential (the upper two graphs in Fig. 2, RSMS code) as well as for calculations which use a self-

consistent potential (the lowermost graph in Fig. 2, ABINIT code). Likewise, similar results are obtained when relying on the muffin-tin approximation (the second graph from the top in Fig. 2), when the muffin-tin approximation is improved via use of additional empty spheres (the uppermost graph) and when the muffin-tin approximation is not used altogether (the lowermost graph). The static effect of the $1s$ core hole as described within the final state approximation is practically negligible — we found that the spectra obtained via the RSMS code for a potential with the core hole can be hardly distinguished from spectra obtained for a ground state potential (not shown here). It is thus evident that the anisotropic damping of XAFS oscillations for energies 20 eV or more above the edge cannot be reproduced by calculations done for a static $(\text{creat})_2\text{CuCl}_4$ crystal.

As concerns individual spectra, our calculations are unable to reproduce correctly the peak intensities within the first 10 eV above the absorption edge. We conjecture that this is connected with many-body effects beyond the local density approximation (LDA). Let us recall in this regard the discussion about whether the Cu K edge XANES of complexes containing linear or square-planar CuCl_n units is dominated by many-body (mostly shake-down) features or whether it is dominated by hybridisation between states of neighbouring CuCl_n units.^{30–32,36} Similar arguments are also put forward in connection with XANES of copper oxides.^{13–15,33–35,37} To contribute to this debate is beyond our scope but we would like to point out that approaches which handle local many-body effects accurately via quantum chemistry configuration interaction calculations are usually unable to consider the interaction between neighbouring CuCl_n units while calculations which include this long-range interaction treat the many-body effects only in a mean-field way (via the LDA). Assessing the relative importance of both contributions is thus difficult. The failure of our calculations to reproduce the experiment accurately down to the edge can be seen as an evidence that many-body effects are important in this region but we cannot conclude whether they are dominant or not.

Interestingly, the shape of the broad $\varepsilon \parallel z$ peak around 20–30 eV cannot be described accurately unless a self-consistent non-muffin-tin potential is used: the three sub-peaks this feature consists of are well reproduced by ABINIT calculations but not by RSMS calculations. It appears thus that disregarding the topic of the anisotropic XAFS damping, the states lying predominantly in the xy crystallographic plane which contains a lot of atoms are well-described by the non-self-consistent muffin-tin potential, while the states in the more-or-less empty interstitial region between the CuCl_4 -planes can be described properly only if the approximations laid on the potential are relaxed. This is plausible — one expects that the muffin-tin approximation will be more crude in empty regions than in regions packed with atoms.

Finally, we should mention that our theoretical spectra do not exhibit the weak pre-edge structure which appears

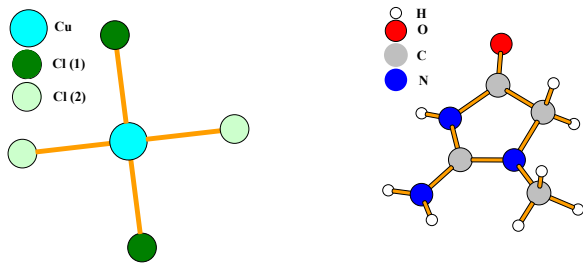


FIG. 3. Molecular blocks forming the $(\text{creat})_2\text{CuCl}_4$ crystal.

in the experiment around zero eV in the scale of Fig. 2 (x-ray energies about 8978 eV). Our calculations are based on the dipole selection rule, reflecting thus only states having the p symmetry with respect to the Cu atoms. The pre-edge structure, on the other hand, is to a large extent formed by quadrupole transitions, reflecting thus the d states. Another contribution to the pre-edge structure may come from dipole transitions allowed by vibrational symmetry breaking. The role of quadrupole transitions for the Cu K pre-edge structure was discussed widely in the past^{13,29,54} and the same is true for the effect of vibrations on pre-edge intensities.^{10,12} We want to focus rather on the higher-energy part of the spectrum.

B. Influence of vibrations

Because static lattice calculations were not able to reproduce the large difference between the damping of XAFS oscillations for the $\varepsilon \parallel z$ and for $\varepsilon \perp z$ polarisations, we performed another set of calculations, accounting this time for vibrations by the method described in Sec. II A. The occurrence of the anisotropic damping of XAFS in the experiment suggests that one should consider different MSRD's for different bonds. This means that we have to identify which interatomic distances will be regarded as stiff and which will be regarded as soft. By inspecting the $(\text{creat})_2\text{CuCl}_4$ structure one can realize that the $(\text{creat})_2\text{CuCl}_4$ crystal is actually formed by creatinium and CuCl_4 molecular units which are relatively independent (they are linked through N-H...Cl hydrogen bonding).⁵⁵ These units are displayed in Fig. 3. We assume that if two atoms belong to the same molecular unit, their interatomic distance is characterised by a small MSRD which we denote σ_{idd}^2 . If two atoms belong to different molecular units, their interatomic distance is characterised by a large MSRD, denoted as σ_{diff}^2 . At the moment, we have no clear indication how to chose the values of σ_{idd}^2 and σ_{diff}^2 , therefore we treat them as model parameters and set their values in accordance with what was reported for other systems in the literature. Our goal is to check whether a model based on the substitution of Eq. (3) with two distinct σ^2 parameters can simulate the anisotropic XAFS damping which we observe for $(\text{creat})_2\text{CuCl}_4$.

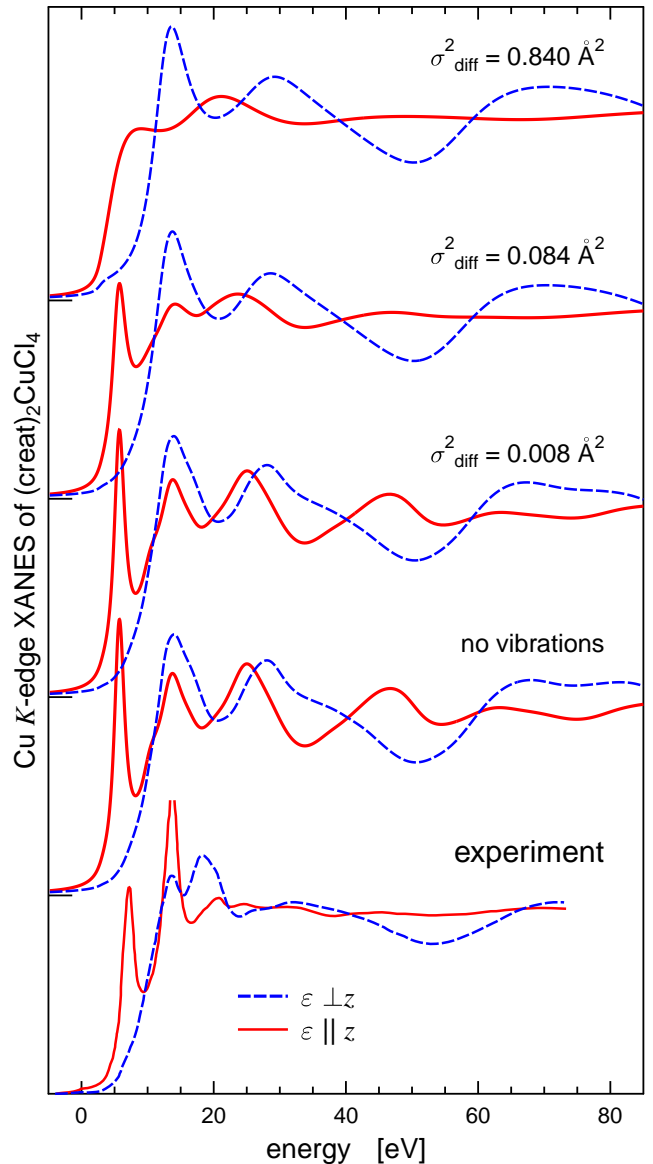


FIG. 4. Theoretical Cu K edge XANES of $(\text{creat})_2\text{CuCl}_4$ calculated while including the vibrational disorder, compared to the static lattice calculation and to the experiment.

We performed a set of calculations with a fixed $\sigma_{\text{idd}}^2=0.0008 \text{ \AA}^2$ while varying σ_{diff}^2 as 0.008, 0.084, and 0.840 \AA^2 . These results are compared with results for a static lattice and with the experimental data (Fig. 4). One can see that if we take $\sigma_{\text{diff}}^2=0.084 \text{ \AA}^2$, the XAFS oscillations for the $\varepsilon \parallel z$ component are strongly damped for x-ray energies above 20–30 eV, as required. A substantially lower σ_{diff}^2 does not lead to the desired damping while a substantially larger σ_{diff}^2 results in overdamping of the oscillations at low energies. We can thus conclude that our way of including the vibrations in the XANES calculations, together with the scheme for assigning σ_{idd}^2 and σ_{diff}^2 to atomic pairs depending on whether they belong to the same molecular unit or not, is a good approximation to describe the mechanism of the anisotropic damping of XAFS for $(\text{creat})_2\text{CuCl}_4$.

IV. DISCUSSION

Our goal was to examine whether a technically simple method to account for the effect of vibrations in XANES calculation by modifying the free-electron propagator can be useful in analysing XAFS in certain systems. By analysing theoretical Cu K edge spectra of $(\text{creat})_2\text{CuCl}_4$ obtained for static and vibrating systems we were able to link the differences in the damping of experimental XAFS oscillations for the in-plane and out-of-plane polarisations to the differences in MSRD's according to whether the respective atoms belong to the same molecular unit or not.

The MSRD values $\sigma_{\text{idd}}^2=0.0008 \text{ \AA}^2$ and $\sigma_{\text{diff}}^2=0.084 \text{ \AA}^2$ are realistic considering analogous data obtained for similar systems. For example, the MSRD values $\sigma^2(\text{Cu-Cl})=0.0013\text{-}0.0041 \text{ \AA}^2$ in Ref. 56 and 0.008 \AA^2 in Ref. 57 were obtained for the four-fold Cl coordination of copper in chloro-complexes. Note that in these two cases copper atoms are additionally bonded to two oxygen or nitrogen atoms, located at shorter distances than four chlorine atoms. As a result, the Cu-Cl bonding in chloro-complexes is weaker than the Cu-Cl bonding in $(\text{creat})_2\text{CuCl}_4$, and, consequently, the corresponding MSRD's are expected to be larger in chloro-complexes than in $(\text{creat})_2\text{CuCl}_4$.

We can also make a comparison with crystallographic data.⁵⁵ However, one has to bear in mind that in crystallography one deals with disorder in the distribution of atomic displacements measured from a lattice point while in XAS one deals with disorder in the distribution of interatomic distances. Correlations between movements of atoms are responsible for the differences between crystallographic σ_{cryst}^2 and XAS-related σ_{XAS}^2 . Crystallographic data suggest that the vibrations of all atoms in $(\text{creat})_2\text{CuCl}_4$ are strongly anisotropic: σ_{cryst}^2 along the z axis is up to four times larger than σ_{cryst}^2 within to the xy plane.⁵⁵ This is consistent with our picture, because small “intra-block” vibrations associated with σ_{idd}^2 will be mostly in the xy plane while large “inter-block” vibrations associated with σ_{diff}^2 will be both in the xy plane and along the z axis. If the correlations are neglected, an estimate for pair-wise σ_{XAS}^2 can be obtained by summing the crystallographic σ_{cryst}^2 values for the respective atom pair.⁵⁵ If we do this for the Cu-X pairs along the z axis, where only weak correlations can be expected, we get $\sigma_{\text{XAS}}^2=0.10\text{-}0.17 \text{ \AA}^2$. This is comparable with our $\sigma_{\text{diff}}^2=0.084 \text{ \AA}^2$. For vibrations in the xy plane, σ_{cryst}^2 is about $0.05\text{-}0.09 \text{ \AA}^2$ if no correlations are assumed. This is significantly larger than σ_{idd}^2 we use. However, our assumption of the stiffness of individual molecular blocks means that there should be large correlations between movements of respective atoms, so crystallographic σ_{cryst}^2 cannot be directly compared to our σ_{idd}^2 in this respect.

The scheme we employed treats the multiple-scattering in an exact way but the vibrations in an approximative way. However, we do not expect this to have any sig-

nificant influence on our conclusions. As concerns the plane wave approximation laid on the vibrations, it is true that Fujikawa *et al.*²⁰ found a difference in XANES calculated when the vibrations were treated within the spherical wave approximation [Eq. (3.16) in Ref. 20] and when the vibrations were treated within the plane wave approximation [Eq. (3.18) *ibid.*] but this was only for short bond lengths and very large $\sigma^2=0.4 \text{ \AA}^2$. For longer distances, this effect was already very small. In our situation, short bond lengths (between atoms of the same molecular unit) are characterised by small σ^2 , while large σ^2 is associated only with large bond lengths. Hence, the plane wave approximation should be sufficient for the vibrations in this case. As concerns the effect of the vibrations on the scattering phase shifts, the situation is more complicated — earlier studies found some effects in this respect, especially as concerns the higher-order scattering signals.^{4,58} On the other hand, we do not expect this effect to dominate in our situation, because we found that several different potentials lead to similar results in the energy region where the effect of vibrations are visible (see Fig. 2 and the discussion about the pseudopotentials in Sec. II C and about the negligibility of the core hole effect in Sec. III A).

It should be noted that our focus is on the very fact that vibrations give rise to significant observable effects in the polarisation-dependence of $(\text{creat})_2\text{CuCl}_4$ XANES spectra and not on the particular values of σ_{idd}^2 and σ_{diff}^2 . The approximations involved in the model do not allow for taking our σ_{idd}^2 and σ_{diff}^2 values as true best fits. It should be also noted that our splitting of the atomic pairs into the σ_{idd}^2 and σ_{diff}^2 classes is not unique. E.g., the σ_{idd}^2 and σ_{diff}^2 MSRD's could be ascribed to the pairs depending on whether the respective atoms belong to the same layer or not (the layers are depicted figure 1). We did the calculations also for this model and found that the results are almost the same as for the molecular-units-based model. This is not so surprising because atoms belonging to the same unit belong also to the same layer. We also verified that the particular value of $\sigma_{\text{idd}}^2=0.0008 \text{ \AA}^2$ is not crucial — nearly identical results are obtained with a much larger value of $\sigma_{\text{idd}}^2=0.008 \text{ \AA}^2$. Despite the unavoidable ambiguity, we nevertheless assume that the large difference between σ_{idd}^2 and σ_{diff}^2 would be maintained even if a more advanced modelling was employed.

Our interpretation that the polarization-dependence of the XAFS damping in $(\text{creat})_2\text{CuCl}_4$ is a manifestation of the existence of very different MSRD's depending on whether the pair-forming atoms belong to the same basic molecular unit could be confirmed (or refuted) by temperature-dependent measurements of the polarized spectra. If XAFS oscillations for $\varepsilon||z$ are gradually restored when the temperature decreases so that XAFS amplitudes become comparable for $\varepsilon||z$ and $\varepsilon \perp z$, as suggested by static-lattice calculations (see figures 2 and 4), it would be a strong argument in favour of our interpretation.

Generally, our results suggest that whenever one ob-

serves different damping rates of XAFS oscillations for different polarisations, presence of atomic-pair-selective vibrations should be considered. Special attention should be given in this respect to systems where the interatomic distances can be split into different classes according to their presumed stiffness.

The way we include the vibrations into XANES calculations (modifying the free electron propagator) was used before but only to investigate XANES in liquids close to critical conditions and relying on more complicated equations than the simple substitution of Eq. (3).^{24,25} In this work, we focus on a crystal at room temperature and demonstrate that the simple formula (3) can be used to identify vibrational effects in x-ray absorption spectra in the XANES and intermediate energy regions. The same approach could be applied to incorporate vibrations into other spectroscopies that can be described within the real-space multiple-scattering framework (such as, for example, of the x-ray bremsstrahlung isochromat spectroscopy,⁵⁹ x-ray scattering^{60,61} or x-ray photoemission).⁶²

V. CONCLUSIONS

Atomic vibrations can be efficiently incorporated into x-ray absorption spectra calculations based on the multiple-scattering formalism by modifying the free-

electron propagator via a damping factor, $G_{LL''}^{pq} \rightarrow G_{LL''}^{pq} \exp(-k^2 \sigma_{pq}^2)$. If this procedure is used, the effects of vibrations are treated within the same approximations which are involved in the standard EXAFS formula while the multiple scattering itself is treated exactly.

Creatinium tetrachlorocuprate (creat)₂CuCl₄ crystal is an example of a system where the effects of vibrations are significant in the XANES and intermediate energy region (30–100 eV above the edge) even at room temperature. Fine structure oscillations in the experimental Cu *K* edge XAS of (creat)₂CuCl₄ are damped differently for the in-plane and out-of-plane polarisations of the incoming x-rays. The anisotropy of the XAFS damping cannot be reproduced by the theory unless the vibrations are taken into account in such a way that individual molecular blocks within the (creat)₂CuCl₄ crystal are treated as semi-rigid entities while the mutual positions of these blocks are subject to strong relative displacements.

ACKNOWLEDGMENTS

This work was supported by the LD-COST CZ program of the Ministry of Education, Youth and Sport of the Czech Republic within the project LD15097. Stimulating discussions with P. Pattison are gratefully acknowledged.

* sivr@fzu.cz; <http://www.fzu.cz/~sivr>

¹ G. Beni and P. M. Platzman, *Phys. Rev. B* **14**, 1514 (1976).

² R. B. Gregor and F. W. Lytle, *Phys. Rev. B* **20**, 4902 (1979).

³ P. A. Lee, P. H. Citrin, P. Eisenberger, and B. M. Kincaid, *Rev. Mod. Phys.* **53**, 769 (1981).

⁴ M. Benfatto, C. R. Natoli, and A. Filipponi, *Phys. Rev. B* **40**, 9626 (1989).

⁵ J. D. Bourke, C. T. Chantler, and C. Witte, *Phys. Lett. A* **360**, 702 (2007).

⁶ A. Kuzmin and R. A. Evarestov, *J. Phys.: Condens. Matter* **21**, 055401 (2009).

⁷ A. Anspoks, A. Kalinko, R. Kalendarev, and A. Kuzmin, *Phys. Rev. B* **86**, 174114 (2012).

⁸ O. Šipr, G. Dalba, and F. Rocca, *Phys. Rev. B* **69**, 134201 (2004).

⁹ A. Kuzmin, G. Dalba, P. Fornasini, F. Rocca, and O. Šipr, *Phys. Rev. B* **73**, 174110 (2006).

¹⁰ R. V. Vedrinskii, V. L. Kraizman, A. A. Novakovich, P. V. Demekhin, and S. V. Urazhdin, *J. Phys.: Condens. Matter* **10**, 9561 (1998).

¹¹ O. Durmeyer, E. Beaupaire, J.-P. Kappler, C. Brouder, and F. Baudelet, *J. Phys.: Condens. Matter* **22**, 125504 (2010).

¹² D. Manuel, D. Cabaret, C. Brouder, P. Sainctavit, A. Bording, and N. Trcera, *Phys. Rev. B* **85**, 224108 (2012).

¹³ S. Bocharov, T. Kirchner, G. Dräger, O. Šipr, and A. Šimůnek, *Phys. Rev. B* **63**, 045104 (2001).

¹⁴ O. Šipr and A. Šimůnek, *J. Phys.: Condens. Matter* **13**,

8519 (2001).

¹⁵ M. Calandra, J. P. Rueff, C. Gougoussis, D. Ceolin, M. Gorgoi, S. Benedetti, P. Torelli, A. Shukla, D. Chandris, and C. Brouder, *Phys. Rev. B* **86**, 165102 (2012).

¹⁶ N. Dimakis and G. Bunker, *Phys. Rev. B* **58**, 2467 (1998).

¹⁷ A. V. Poiarkova and J. J. Rehr, *Phys. Rev. B* **59**, 948 (1999).

¹⁸ F. D. Vila, J. J. Rehr, H. H. Rossner, and H. J. Krappe, *Phys. Rev. B* **76**, 014301 (2007).

¹⁹ N. Dimakis, T. Mion, and G. Bunker, *J. Phys.: Conf. Ser.* **190**, 012011 (2009).

²⁰ T. Fujikawa, J. Rehr, Y. Wada, and S. Nagamatsu, *J. Phys. Soc. Japan* **68**, 1259 (1999).

²¹ J. J. Rehr and R. C. Albers, *Rev. Mod. Phys.* **72**, 621 (2000).

²² S. Mankovsky, D. Ködderitzsch, G. Woltersdorf, and H. Ebert, *Phys. Rev. B* **87**, 014430 (2013).

²³ P. W. Loeffen and R. F. Pettifer, *Phys. Rev. Lett.* **76**, 636 (1996).

²⁴ K. Hayakawa, K. Kato, T. Fujikawa, T. Murata, and K. Nakagawa, *Jap. J. Appl. Phys.* **38**, 6423 (1999).

²⁵ K. Hayakawa, T. Fujikawa, K. Nakagawa, I. Shimoyama, R. Tittsworth, P. Schilling, and V. Saile, *Chem. Phys.* **289**, 281 (2003).

²⁶ H. Ebert, S. Mankovsky, D. Ködderitzsch, and P. J. Kelly, *Phys. Rev. Lett.* **107**, 066603 (2011).

²⁷ J. J. Rehr, J. J. Kas, F. D. Vila, M. P. Prange, and K. Jorissen, *Phys. Chem. Chem. Phys.* **12**, 5503 (2010).

²⁸ J. J. Rehr, *The FEFF code*, 9, <http://feffproject.org>

- (2013).
- ²⁹ J. Hahn, R. Scott, K. Hodgson, S. Doniach, S. Desjardins, and E. Solomon, *Chem. Phys. Lett.* **88**, 595 (1982).
- ³⁰ N. Kosugi, T. Yokoyama, K. Asakura, and H. Kuroda, *Chem. Phys.* **91**, 249 (1984).
- ³¹ T. Smith, J. Penner-Hahn, M. Berding, S. Doniach, and K. Hodgson, *J. Am. Chem. Soc.* **107**, 5945 (1985).
- ³² T. Yokoyama, N. Kosugi, and H. Kuroda, *Chem. Phys.* **103**, 101 (1986).
- ³³ N. Kosugi, H. Kondoh, H. Tajima, and H. Kuroda, *Chem. Phys.* **135**, 149 (1989).
- ³⁴ J. Guo, D. E. Ellis, G. L. Goodman, E. E. Alp, L. Soderholm, and G. K. Shenoy, *Phys. Rev. B* **41**, 82 (1990).
- ³⁵ A. Bianconi, C. Li, F. Campanella, S. D. Longa, I. Pettiti, M. Pompa, S. Turtù, and D. Udron, *Phys. Rev. B* **44**, 4560 (1991).
- ³⁶ N. Kosugi, in *Chemical Applications of Synchrotron Radiation*, edited by T. S. Sham (World Scientific, Singapore, 2002) p. 228.
- ³⁷ J. Chaboy, A. Munoz-Paez, and E. S. Marcos, *J. Synchr. Rad.* **13**, 471 (2006).
- ³⁸ D. D. Vvedensky, in *Unoccupied Electronic States*, edited by J. C. Fuggle and J. E. Inglesfield (Springer, Berlin, 1992) p. 139.
- ³⁹ C. R. Natoli, M. Benfatto, S. Della Longa, and K. Hatada, *J. Synchr. Rad.* **10**, 26 (2003).
- ⁴⁰ O. Šipr, *Computer code* RSMS, Institute of Physics AS CR, Prague (1996-1999).
- ⁴¹ D. D. Vvedensky, D. K. Saldin, and J. B. Pendry, *Comp. Phys. Commun.* **40**, 421 (1986).
- ⁴² H. Ebert, *Computer code* XBAND 5.0, <http://ebert.cup.uni-muenchen.de/xband> (2008).
- ⁴³ O. Andersen, C. Arcangeli, R. Tank, T. Saha-Dasgupta, G. Krier, O. Jepsen, and I. Dasgupta, in *Tight-binding approach to computational materials science*, Materials Research Society Symposium Proceedings, Vol. 491, edited by P. Turchi, A. Gonis, and L. Colombo (1998) p. 3.
- ⁴⁴ J. Chaboy and S. Quartieri, *Phys. Rev. B* **52**, 6349 (1995).
- ⁴⁵ A. L. Ankudinov, *J. Synchr. Rad.* **6**, 236 (1999).
- ⁴⁶ K. Hatada and J. Chaboy, *Phys. Rev. B* **76**, 104411 (2007).
- ⁴⁷ K. R. Wilson, J. G. Tobin, A. L. Ankudinov, J. J. Rehr, and R. J. Saykally, *Phys. Rev. Lett.* **85**, 4289 (2000).
- ⁴⁸ J. E. Müller, O. Jepsen, and J. W. Wilkins, *Solid State Commun.* **42**, 365 (1982).
- ⁴⁹ M. Benfatto, S. Della Longa, and C. R. Natoli, *J. Synchr. Rad.* **10**, 51 (2003).
- ⁵⁰ X. Gonze, B. Amadon, P. M. Anglade, J. M. Beuken, F. Bottin, P. Boulanger, F. Bruneval, D. Caliste, R. Caracas, M. Cote, T. Deutsch, L. Genovese, P. Ghosez, M. Giantomassi, S. Goedecker, D. R. Hamann, P. Hermet, F. Jollet, G. Jomard, S. Leroux, M. Mancini, S. Mazevet, M. J. T. Oliveira, G. Onida, Y. Pouillon, T. Rangel, G. M. Rignanese, D. Sangalli, R. Shaltaf, M. Torrent, M. J. Verstraete, G. Zerah, and J. W. Zwanziger, *Comp. Phys. Commun.* **180**, 2582 (2009).
- ⁵¹ *Hartwigsen-Goedecker-Hutter type pseudopotentials generated by M. Krack*, <http://cvs.berlios.de/cgi-bin/viewvc.cgi/cp2k/potentials/> (2005).
- ⁵² *Troullier-Martins type pseudopotentials generated by the FHI98PP code*, http://www.abinit.org/downloads/psp-links/psp-links/lda_t (2005).
- ⁵³ *Troullier-Martins type pseudopotentials generated by D. C. Allan and A. Khein*, http://www.abinit.org/downloads/psp-links/psp-links/lda_t (2005).
- ⁵⁴ Z. Y. Wu, D. C. Xian, T. D. Hu, Y. N. Xie, Y. Tao, C. R. Natoli, E. Paris, and A. Marcelli, *Phys. Rev. B* **70**, 033104 (2004).
- ⁵⁵ M. Udupa and B. Krebs, *Inorg. Chim. Acta* **33**, 241 (1979).
- ⁵⁶ M. Tanimizu, Y. Takahashi, and M. Nomura, *Geochem. J.* **41**, 291 (2007).
- ⁵⁷ L. Ivashkevich, A. Kuzmin, D. Kochubei, V. Kriventsov, A. Shmakov, A. Lyakhov, V. Efimov, S. Tyutyunnikov, and O. Ivashkevich, *J. Surf. Investig. X-ray, Synchrotr. Neutron Techniq.* **2**, 641 (2008).
- ⁵⁸ T. Yokoyama and T. Ohta, *J. Phys. Soc. Japan* **65**, 3909 (1996).
- ⁵⁹ A. Šimůnek, O. Šipr, and J. Vackář, *Phys. Rev. Lett.* **63**, 2076 (1989).
- ⁶⁰ T. Fujikawa, T. Konishi, and T. Fukamachi, *J. Electron. Spectrosc. Relat. Phenom.* **134**, 195 (2004).
- ⁶¹ J. J. Kas, J. J. Rehr, J. A. Soininen, and P. Glatzel, *Phys. Rev. B* **83**, 235114 (2011).
- ⁶² T. Fujikawa, *J. Electron. Spectrosc. Relat. Phenom.* **173**, 51 (2009).